Lifetimes of magnetic-rotational bands in ^{196}Pb

A. K. Singh, H. Hübel, D. Roßbach, S. Chmel, A. Görgen,* E. Mergel, and G. Schönwaßer
Institut für Strahlen- und Kernphysik, Universität Bonn, Nussallee 14-16, D-53115 Bonn, Germany

F. Azaiez and C. Bourgeois
IPN Orsay, IN2P3/CNRS, F-91406 Orsay, France

F. Hannachi, A. Korichi, and A. Lopez-Martens
CSNSM Orsay, IN2P3/CNRS, F-91405 Orsay, France

A. Astier, N. Buforn, N. Redon, and O. Stezowski
IPN Lyon, IN2P3/CNRS, Université Lyon-1, F-69622 Villeurbanne, France

D. Bazzacco, T. Kröll, and C. Rossi-Alvarez
Dipartimento di Fisica and INFN, Università di Padova, I-35131 Padova, Italy

K. Hauschild, W. Korten, and R. Lucas
CEA Saclay, DAPNIA/SPhN, F-91191 Gif sur Yvette, France

H. J. Maier, P. Reiter, and P. G. Thirolf
Sektion Physik, Ludwig-Maximilians-Universität München, Am Coulombwall 1, D-85748 Garching, Germany

A. N. Wilson†
Department of Physics, University of York, York YO10 5DD, United Kingdom
(Received 8 July 2002; published 13 December 2002)

Lifetimes have been measured for states in four magnetic-rotational bands in ^{196}Pd using the Doppler-shift attenuation method. Line shapes of several transitions in each band have been analyzed in γ-ray coincidence spectra measured with the EUROBALL spectrometer array. The $B(M1)$ values deduced from the lifetimes show a decrease with increasing spin within the bands as expected for the shears mechanism. The $B(M1)$ values are compared to calculations within the framework of the tilted-axis cranking model.

DOI: 10.1103/PhysRevC.66.064314 PACS number(s): 21.10.Tg, 23.20.Lv, 27.80.+w

I. INTRODUCTION

In many near-spherical nuclei rotational cascades of strongly enhanced magnetic dipole ($M1$) transitions have been observed in recent years [1,2]. These $M1$ bands occur when the symmetry is broken by the current distributions of a few high-spin particles and holes outside a near-spherical core and by the magnetic moments associated with these currents [3–7]. The particle-hole interaction is repulsive; because of this, the lowest energy is obtained for a perpendicular coupling of the particle and hole orbitals. This is the configuration of the bandhead [4]. The perpendicular coupling of the proton-particle and neutron-hole (or vice versa) spins gives rise to a large component of the magnetic moment perpendicular to the total angular momentum. This component of the magnetic moment is responsible for the strongly enhanced $M1$ radiation. Since it is a magnetic moment that breaks the symmetry and rotates around the angular momentum vector, this mode of nuclear excitation has been called ‘‘magnetic rotation’’ [5,6]. This is very different from the conventional rotation of a deformed charge distribution that gives rise to bands of enhanced $E2$ radiation.

Within the magnetic-rotational bands angular momentum and excitation energy are increased by a step-by-step alignment of the particle and hole spins into the direction of the total spin [3–7]. Since this resembles the closing of a pair of shears, the $M1$ bands have also been called ‘‘shears bands’’ [3]. A consequence of the shears effect is a decrease of the perpendicular component of the magnetic moment and, thus, a well defined decrease of the $B(M1)$ values with increasing angular momentum in the bands [6,8]. This decrease of the $B(M1)$ values, which is considered to be the clearest signature of the shears mechanism, has been observed experimentally for $M1$ bands in different mass regions [8–17]; however, lifetimes have generally only been measured for the most strongly populated band in each isotope.

In our recent spectroscopic investigation of ^{196}Pb [18] using the EUROBALL γ-ray spectrometer array [19] we have established nine magnetic-rotational bands in that nucleus. In this paper, we report on a Doppler-shift attenuation method (DSAM) analysis of lifetimes of states in four of these bands. For the remaining bands a lifetime analysis was not possible due to the lack of sufficient uncontaminated energy gates to produce clean γ-ray coincidence spectra or a lack of statisti-

*Present address: Nuclear Science Division, Lawrence Berkeley Nat. Lab., Berkeley, CA 94720.

†Present address: Department of Nuclear Physics, RSPhS, ANU, Canberra ACT 0200, Australia.

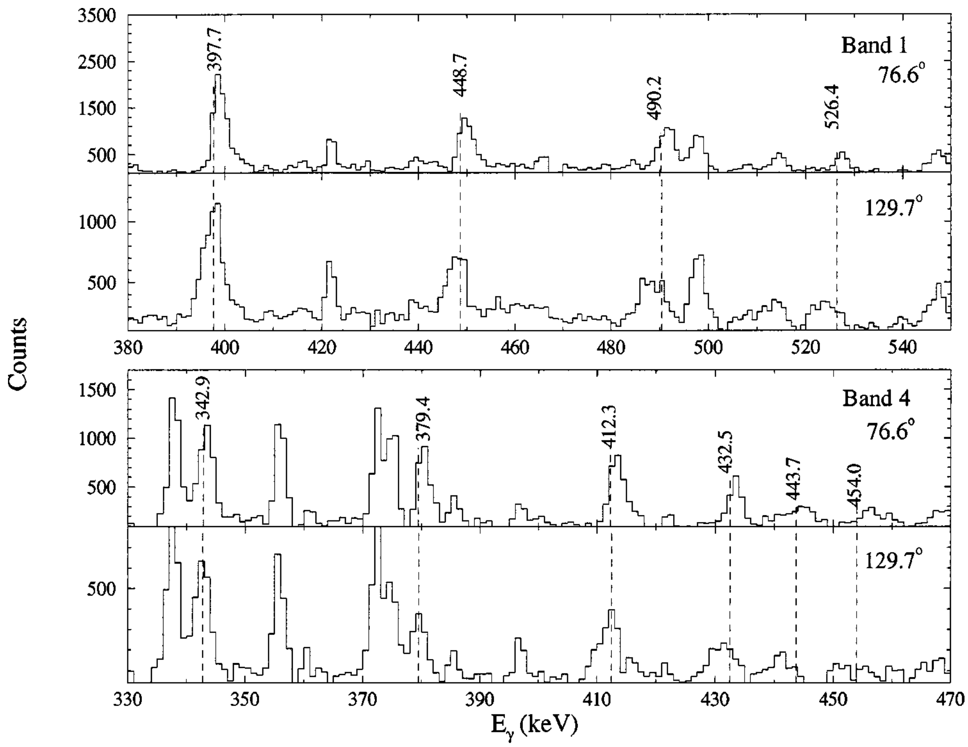

FIG. 1. Gamma-ray coincidence spectra showing line shapes of transitions of band 1 (upper panel, triple-gated spectrum) and band 4 (lower panel, double-gated spectrum) in ^{196}Pb (Ref. [18]) measured at 76.6° and 129.7°.

cal accuracy. It was the aim of this investigation to verify whether the $B(M1)$ values deduced from the lifetimes show the characteristic decrease expected for shears bands.

In the following section the experimental methods and results are described; these results are then discussed and compared to tilted-axis cranking (TAC) calculations in Sec. III.

II. EXPERIMENTAL METHODS AND RESULTS

High-spin states in ^{196}Pb were populated using the reaction ^{170}Er(^{30}Si,4n). The ^{30}Si beam of 144 MeV was provided by the Vivitron tandem accelerator at the Institut de Recherches Subatomiques at Strasbourg. An enriched ^{170}Er foil of 1.65 mg/cm^2 thickness on a 6.64 mg/cm^2 thick Au backing was used as a target. Coincidences between the emitted γ rays were measured with the EUROBALL spectrometer array [19]. It comprises 30 Compton-suppressed conventional (tapered) Ge detectors and 41 composite Ge detectors. Of the latter, the 26 Clover detectors are composed of four Ge crystals each and the 15 Cluster detectors consist of seven Ge crystals each. At the time of the experiment, 230 individual Ge crystals out of the total of 239 crystals of the full array could be used. An inner ball of 210 BGO scintillation detectors was used as a multiplicity filter. Coincidence events were written to tape when four or more Ge crystals before Compton suppression and five or more BGO detectors showed a signal. In the presorting of the data gain matching, pile-up suppression, Compton suppression, and add-back for the composite detectors were carried out. After setting a window on the prompt time peak, a total of 1.1×10^9 events with γ-ray coincidence fold greater than or equal to 3 remained for further analysis.

The Ge crystals of the EUROBALL spectrometer array can be grouped into eight rings at the following average angles with respect to the beam direction: 15.5°, 34.6°, 52.3°, 76.6°, 103.3°, 129.7°, 137.1°, and 156.2°. For each of these angles γ-ray coincidence spectra were produced by setting double or triple gates on the transitions in the low-spin part of the bands which were emitted after the nuclei had come to rest in the Au backing. Background corrected spectra which were obtained by subtracting a fraction of the spectrum with the next lower coincidence fold were used for the line-shape analysis. Figure 1 shows examples of such spectra from forward and backward detectors of bands 1 and 4. The spectra are not symmetrical due to the different detector types under forward (tapered Ge) and backward (Cluster) angles in the EUROBALL array. In the intermediate-energy region of the bands, typically for transition energies between 300 and 500 keV, the Doppler-shifted line shapes could be analyzed. Spectra from the near-90° detectors were used to locate possible contaminations at the position of the shifted peaks in the spectra from the forward and backward detectors. Sufficiently clean spectra for a line-shape analysis could be observed for bands 1, 4, 7, and 8 of ^{196}Pb [18]. In order to obtained sufficient statistics, it was necessary to work with spectra created by setting gates on transitions below the transitions for which the lifetimes were to be determined. For this reason, the side-feeding lifetimes had to be taken into account; the side-feeding model used in the analysis is described below.

Line shapes were calculated and fitted to the experimental spectra using the program developed by Bacelar *et al.* [20] and modified by Gascon *et al.* [21]. In the first step of the calculation, a Monte Carlo simulation of 5000 histories of nuclei recoiling through the target and stopper foils is performed. Starting with the initial recoil velocity of $v/c = 1.53\%$, calculated for the center of the target, this results

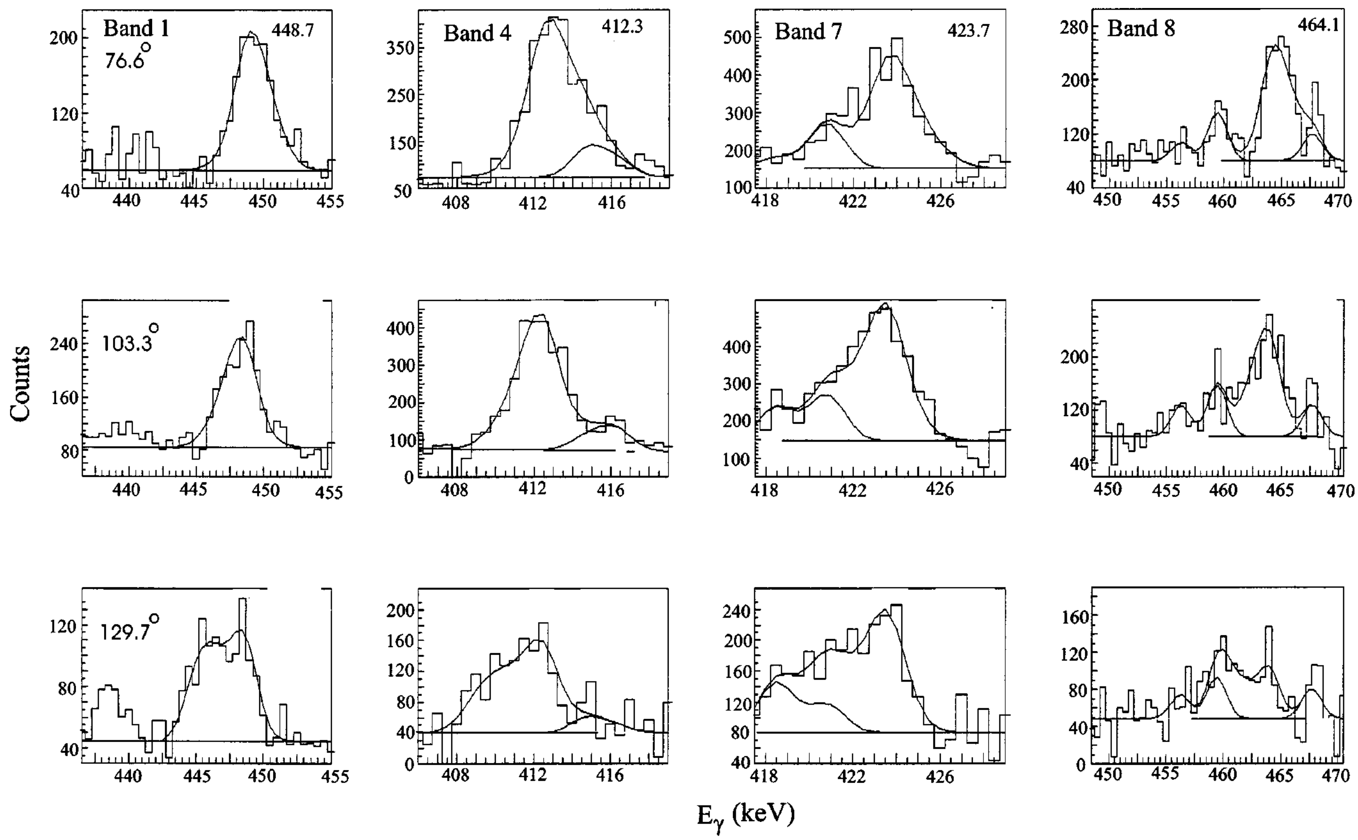

FIG. 2. Examples of experimental and calculated line shapes for γ-ray transitions belonging to bands 1, 4, 7, and 8 for forward, near-90°, and backward angles. Fits to contaminations are included. The shape of the contaminant for the 423.7 keV γ ray of band 7 is different in the different angle spectra due to the presence of the short-lived 420.8 keV γ ray at higher spin in the same band (Ref. [18]) which shows different line shapes at the different angles.

in statistical velocity distributions of about 720 different times with time intervals of 2 fs. In the second step, the details of the detector geometry are taken into account and a line shape is calculated for each decay time, using the velocity distributions from the first step of the calculation and the stopping powers. The electronic stopping powers were calculated using the tables of Northcliffe and Schilling [22], corrected for shell effects. The nuclear contribution was treated according to the prescription given by Lindhard *et al.* [23]. Finally, the calculated line shapes were fitted to the experimental ones with the lifetimes as free parameters. The side feeding was modeled by a rotational cascade of five transitions with a moment of inertia typical of that of the investigated $M1$ bands in a spin region where they show no crossing. Calculations were also performed with different moments of inertia for the side-feeding cascade, but it was found that the level lifetimes were not sensitive to this parameter. The intensities of the side-feeding transitions into each level were obtained from the difference of measured intensities of the γ-ray transitions populating and depopulating the level of interest.

In the line-shape fitting procedure, spectra from three different angle groups of forward, near-90°, and backward detectors were always used simultaneously. The results from different combinations of these angle groups were in agreement within the limits of error and final values for the lifetimes for the levels were obtained by taking averages from the different fits. In the fits the in-band and side-feeding lifetimes, the background, and contamination parameters for each transition were allowed to vary. The calculated line shapes were fitted to experimental spectra by a χ^2-minimization procedure, starting with the highest transition of a cascade. The effective lifetime of the highest level was then fixed and used as the in-band feeding time for the next lower level. In addition, a global fit for all the transitions of a cascade with independent in-band and side-feeding lifetimes was performed. Examples of the fits of calculated line shapes to experimental spectra are shown in Fig. 2.

Lifetimes of states in four magnetic-rotational bands in ^{196}Pb, bands 1, 4, 7, and 8 [18], have been determined. We were unable to extract reliable results for the other bands in this nucleus either because of poor statistics or because of contaminations in the spectra. In band 1 we could not measure lifetimes of transitions below the 27^+ state due to presence of intense unshifted γ rays from low-lying levels of energy close to that of the band. The side-feeding lifetimes were varied within reasonable limits (about 10%) around the values obtained from the lowest-χ^2 fits to determine the influence on the in-band lifetimes. It was found that the uncertainties of the in-band lifetimes due to changes in the side-feeding lifetimes diminish for the transitions lower down in the band. The lifetimes of the transitions of the side-feeding

TABLE I. Measured lifetimes τ and reduced transition probabilities $B(M1)$ and $B(E2)$ of states of magnetic-rotational bands in ^{196}Pb. Side-feeding intensities I_{sf} and the branching ratio B_γ (see text) are also given.

	E_γ^{M1} (keV)	I_{sf} (%)	E_γ^{E2} (keV)	B_γ	τ (ps)	$B(M1)$ (μ_N^2)	$B(E2)$[a] (e^2b^2)
Band 1	526.4	45(11)	1016.6	0.81(6)	$0.16^{+0.03}_{-0.03}$	$1.80^{+0.36}_{-0.36}$	$0.078^{+0.031}_{-0.031}$
	490.2	33(8)	938.9	0.83(5)	$0.13^{+0.03}_{-0.03}$	$2.75^{+0.66}_{-0.66}$	$0.131^{+0.054}_{-0.054}$
	448.7	42(7)	846.4	0.83(5)	$0.14^{+0.02}_{-0.02}$	$3.24^{+0.50}_{-0.50}$	$0.191^{+0.063}_{-0.063}$
	397.7	51(10)	736.4	0.89(2)	$0.13^{+0.03}_{-0.02}$	$5.12^{+0.80}_{-1.19}$	$0.269^{+0.082}_{-0.094}$
Band 4	454.0	39(10)			$0.13^{+0.03}_{-0.02}$	$4.08^{+0.63}_{-0.94}$	
	443.7	27(8)			$0.11^{+0.02}_{-0.02}$	$5.12^{+0.93}_{-0.93}$	
	432.5	27(9)			$0.14^{+0.03}_{-0.02}$	$4.30^{+0.61}_{-0.92}$	
	412.3	36(10)			$0.13^{+0.03}_{-0.02}$	$5.24^{+0.81}_{-1.21}$	
	379.4	35(9)			$0.15^{+0.03}_{-0.02}$	$5.60^{+0.75}_{-1.12}$	
	342.9	26(6)			$0.17^{+0.03}_{-0.03}$	$6.30^{+1.11}_{-1.11}$	
Band 7	362.8	27(9)			$0.15^{+0.03}_{-0.03}$	$6.26^{+1.25}_{-1.25}$	
	413.7	26(8)			$0.20^{+0.04}_{-0.04}$	$3.38^{+0.56}_{-0.56}$	
	423.7	35(8)			$0.16^{+0.03}_{-0.03}$	$3.97^{+0.75}_{-0.75}$	
	348.8	40(8)			$0.16^{+0.04}_{-0.03}$	$6.45^{+1.19}_{-1.59}$	
Band 8	513.2	34(12)			$0.14^{+0.03}_{-0.03}$	$2.72^{+0.58}_{-0.58}$	
	464.1	33(10)			$0.14^{+0.03}_{-0.02}$	$3.57^{+0.51}_{-0.77}$	
	399.5	39(10)			$0.13^{+0.02}_{-0.02}$	$5.68^{+0.87}_{-0.87}$	
	339.3	28(8)			$0.15^{+0.03}_{-0.02}$	$7.37^{+0.98}_{-1.47}$	
	289.0	22(6)			$0.23^{+0.04}_{-0.04}$	$6.84^{+1.19}_{-1.19}$	

[a]Calculated from $B(M1)/B(E2)$ ratios obtained from Ref. [18].

cascade with similar energies as those of the $M1$ band are comparable to the in-band lifetimes. The results for the lifetimes of states in the four $M1$ bands that could be analyzed are summarized in Table I. The quoted errors include the statistical and systematic uncertainties, determined as described above, but do not include the systematic errors introduced through the treatment of the stopping power which may be as large as 10%–15%.

III. DISCUSSION

From the lifetimes presented above reduced transition probabilities can be obtained for high-spin states in the magnetic-rotational bands 1, 4, 7, and 8 in ^{196}Pb. The reduced $M1$ transition probabilities, $B(M1)$, were calculated assuming that the $\Delta I=1$ in-band transitions are of pure $M1$ character. A small $E2$ admixture (δ) would not influence the results since it enters as δ^2 in the analysis. For band 1, $\Delta I=2$ crossover transitions were observed and the branching ratios $B_\gamma=I_\gamma(\Delta I=1)/[I_\gamma(\Delta I=1)+I_\gamma(\Delta I=2)]$ were adopted from Ref. [18]. The total $M1$ conversion coefficients were taken from Ref. [24]. The resulting $B(M1)$ values are summarized in Table I. Figure 3 presents plots of these values as a function of spin for all four bands. Band 7 is not linked to lower-lying states and its configuration is therefore

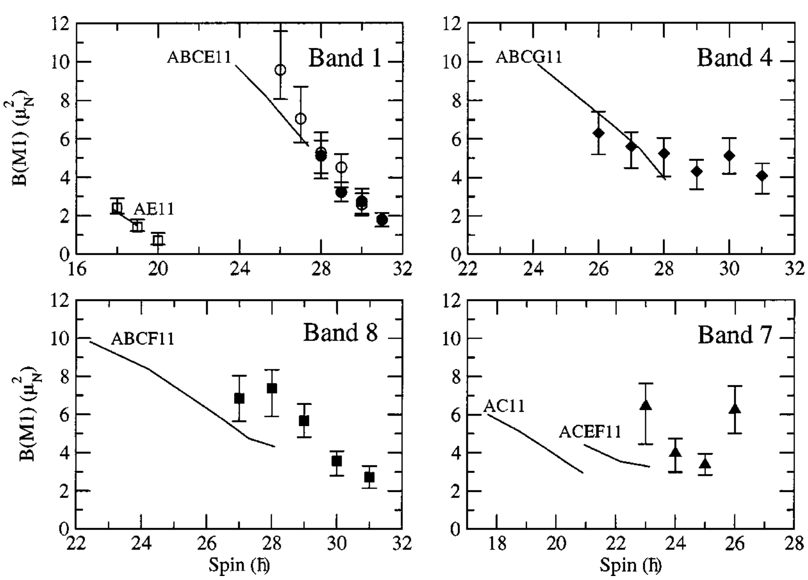

FIG. 3. Experimental $B(M1)$ values for bands 1, 4, 7, and 8 in ^{196}Pb. Calculations within the framework of the TAC model are included for the configurations of the bands suggested in Ref. [18]. For band 1 previous results (Refs. [10,12]) are shown by open symbols. For band 7 the spin assignments are tentative (Ref. [18]).

uncertain. The spin values adopted in Fig. 3 are suggested by the decay pattern of the band.

For band 1 lifetimes have been measured previously in the lower part of the band, below the band crossing, and in the upper part of the band, above the crossing, by the Doppler-shift recoil-distance method [12] and the DSAM [10], respectively. The $B(M1)$ deduced from the previously measured lifetimes are included in Fig. 3. Our results for the high-spin region of band 1 are in agreement with these values.

Configuration assignments have been made previously [18] for the bands in ^{196}Pb on the basis of their excitation energies, spins, parities, and systematic behavior as well as by comparison to TAC model calculations. The nomenclature is adopted from the work of Baldsiefen *et al.* [3], where quasineutron orbitals are labeled according to the cranked shell model by letters *A*,*B*, . . . , and the proton excitation is given by its spin quantum number. In the four bands investigated in this work, the proton contribution to the configuration is the $\pi(h_{9/2}i_{13/2})11^-$ excitation. This particlelike excitation is coupled to different quasineutron-hole excitations. For the occurrence of the magnetic-rotational bands the high-spin quasineutron holes (*A*,*B*,*C*) of $\nu i_{13/2}$ origin are of importance. At the bandhead the high-spin particles and holes couple with their orbitals approximately perpendicular for a maximum overlap of their density distributions. Within the bands, energy and spin are increased by the shears effect [3].

The experimentally observed decrease of the $B(M1)$ values with increasing spin within the bands is a direct consequence of the shears effect. As the proton and neutron spins align step by step with the direction of the total angular momentum, the component of the magnetic moment that is perpendicular to the total spin, $\mu_\perp$, decreases. Since this component of the magnetic moment is responsible for the $M1$-transition strength, the $B(M1)$ values have to decrease with increasing spin within the bands. However, a smooth decrease is only expected within a band if the configuration does not change. In spin regions where configuration changes occur the transition strength can vary drastically. This is clearly demonstrated in Fig. 3 by the large difference of $B(M1)$ values of band 1 below and above the *BC* alignment. Band 4 shows an alignment around spin $30\hbar$ [18] and the configuration change is also reflected by the larger $B(M1)$ values in that spin range. As mentioned above, the configuration assignment for band 7 is tentative [18]. The increase in $B(M1)$ observed at a tentative spin of $26\hbar$ is caused by a configuration change which causes a backbending in that spin range [18].

In the past the TAC model [5,6] has been applied to calculate properties of the shears bands. Compared to our previous calculations [3,8], we have made the following changes: (i) the TAC quadrupole-quadrupole coupling constant was adjusted to reproduce the experimental quadrupole moment of the 12^+ isomer in ^{196}Pb [25]; and (ii) the deformation within the bands, which was kept fixed previously, was calculated self-consistently as a function of rotational frequency for each configuration. The $B(M1)$ values calculated in this way for the four-quasineutron-hole/two-proton configurations suggested for the bands [18] are included in Fig. 3. As can be seen, the overall slope of the decrease of the $B(M1)$ values is reproduced reasonably well by the calculations. However, for bands 7 and 8 the absolute values underestimate the experimental results. This discrepancy may be either due to uncertainties of the calculations or due to the configuration assignments, in particular for band 7, which is not connected to lower-lying levels [18].

A comparison of the $B(M1)$ values of the four bands shows that they are rather similar. This is expected for bands based on similar configurations. Bands 1, 4, and 8 all have three quasineutrons of $\nu i_{13/2}$ origin and one natural-parity quasineutron of $p_{3/2}f_{5/2}$ origin coupled to the $\pi(h_{9/2}i_{13/2})11^-$ excitation in their configuration. For band 7 the tentatively suggested configuration [18] differs from those of the other bands as it probably involves only two $i_{13/2}$ quasineutrons. The main contribution to the magnetic moment stems from the proton excitation, which is the same in all four bands. Its component perpendicular to the nuclear spin, $\mu_\perp$, determines the size of the $B(M1)$ values. Thus, the observed size and the decrease should be similar in all four bands, despite the difference in neutron excitations. The decrease is also a direct confirmation of the shears effect [3]. Although small decreases of $B(M1)$ values may occur in $M1$ bands based on high-*K* multiquasiparticle states, the reductions observed here can only be explained by involving the shears concept. This observation agrees with previous results for the strongest magnetic-rotational bands in a series of Pb isotopes with mass numbers between 194 and 199 [8–12].

IV. SUMMARY

To summarize, we have measured lifetimes of states in four magnetic-rotational bands in ^{196}Pb. Doppler-broadened line shapes in γ-ray coincidence spectra measured with the EUROBALL spectrometer have been analyzed. The deduced $B(M1)$ values show a decrease with increasing angular momentum, as expected for the shears effect. $B(M1)$ values calculated within the framework of the TAC model reproduce the qualitative behavior reasonably well. Together with previous analyses of $B(M1)$ values in neighboring isotopes, the data support the suggestion that the shears mechanism is responsible for the generation of angular momentum with increasing energy within these $M1$ bands.

ACKNOWLEDGMENTS

We wish to thank the staff of the Strasbourg accelerator for providing the beam and we greatly appreciate the technical support in running the EUROBALL spectrometer. One of us, A.K.S., acknowledges financial support from the A. v. Humboldt foundation. The work was supported by BMBF (Germany) under Contract No. 06BN907. Support by the EU under Contract Nos. ERBFMGECT980145, ERBFMGECT970123, and HPRICT199900079 is gratefully acknowledged.

[1] R. B. Firestone, in *Table of Isotopes*, edited by V. S. Shirley, C. M. Baglin, S. Y. F. Chu, and J. Zipkin (Wiley, New York, 1996).
[2] Amita, A. K. Jain, and B. Singh, At. Data Nucl. Data Tables **74**, 283 (2000).
[3] G. Baldsiefen, H. Hübel, W. Korten, D. Mehta, N. Nenoff, B. V. Thirumala Rao, P. Willsau, H. Grawe, J. Heese, H. Kluge, K. H. Maier, R. Schubart, S. Frauendorf, and H. J. Maier, Nucl. Phys. **A574**, 521 (1994).
[4] S. Chmel, F. Brandolini, R. V. Ribas, G. Baldsiefen, A. Görgen, M. De Poli, P. Pavan, and H. Hübel, Phys. Rev. Lett. **79**, 2002 (1997).
[5] S. Frauendorf, Z. Phys. A **358**, 163 (1997).
[6] S. Frauendorf, Rev. Mod. Phys. **73**, 463 (2001).
[7] R. M. Clark and A. O. Macchiavelli, Annu. Rev. Nucl. Part. Sci. **501**, 1 (2000).
[8] M. Neffgen, G. Baldsiefen, S. Frauendorf, H. Grawe, J. Heese, H. Hübel, H. Kluge, A. Korichi, W. Korten, K. H. Maier, D. Mehta, J. Meng, N. Nenoff, M. Piiparinen, M. Schönhofer, R. Schubart, U. J. van Severen, N. Singh, G. Sletten, B. V. Thirumala Rao, and P. Willsau, Nucl. Phys. **A595**, 499 (1995).
[9] R. M. Clark, S. J. Asztalos, G. Baldsiefen, J. A. Becker, L. Bernstein, M. A. Deleplanque, R. M. Diamond, P. Fallon, I. M. Hibbert, H. Hübel, R. Krücken, I. Y. Lee, A. O. Macchiavelli, R. W. MacLeod, G. Schmid, F. S. Stephens, K. Vetter, R. Wadsworth, and S. Frauendorf, Phys. Rev. Lett. **78**, 1868 (1997).
[10] R. M. Clark, R. Krüken, S. J. Asztalos, J. A. Becker, B. Busse, S. Chmel, M. A. Deleplanque, R. M. Diamond, P. Fallon, D. Jenkins, K. Hauschild, I. M. Hibbert, H. Hübel, I. Y. Lee, A. O. Macchiavelli, R. W. MacLeod, G. Schmid, F. S. Stephens, U. J. van Severen, K. Vetter, R. Wadsworth, and S. Wan, Phys. Lett. B **440**, 251 (1998).
[11] R. Krücken, R. M. Clark, A. Dewald, M. A. Deleplanque, R. M. Diamond, P. Fallon, K. Hauschild, I. Y. Lee, A. O. Macchiavelli, R. Peusquens, G. J. Schmid, F. S. Stephens, K. Vetter, and P. von Brentano, Phys. Rev. C **58**, R1876 (1998).
[12] G. Kemper, A. Dewald, I. Wiedenhöver, R. Peusquens, S. Kasemann, K. O. Zell, P. von Brentano, H. Hübel, S. Chmel, A. Görgen, D. Bazzacco, R. Venturelli, S. Lunardi, D. R. Napoli, F. Hannachi, A. Lopez-Martens, R. Krücken, J. R. Cooper, R. M. Clark, M. A. Deleplanque, I. Y. Lee, A. O. Machiavelli, and F. S. Stephens, Eur. Phys. J. A **11**, 121 (2001).
[13] R. M. Clark, S. J. Asztalos, B. Busse, C. J. Chiara, M. Cromaz, M. A. Deleplanque, R. M. Diamond, P. Fallon, D. B. Fossan, D. G. Jenkins, S. Juutinen, N. Kelsall, R. Krücken, G. J. Lane, I. Y. Lee, A. O. Macchiavelli, R. W. MacLeod, G. Schmid, J. M. Sears, J. F. Smith, F. S. Stephens, K. Vetter, R. Wadsworth, and S. Frauendorf, Phys. Rev. Lett. **82**, 3220 (1999).
[14] D. G. Jenkins, R. Wadsworth, J. A. Cameron, R. M. Clark, D. B. Fossan, I. M. Hibbert, V. P. Janzen, R. Krücken, G. J. Lane, I. Y. Lee, A. O. Macchiavelli, C. M. Parry, J. M. Sears, J. F. Smith, and S. Frauendorf, Phys. Rev. Lett. **83**, 500 (1999).
[15] N. S. Kelsall, R. Wadsworth, S. J. Asztalos, B. Busse, C. J. Chiara, R. M. Clark, M. A. Deleplanque, R. M. Diamond, P. Fallon, D. B. Fossan, D. G. Jenkins, S. Juutinen, R. Krücken, G. J. Lane, I. Y. Lee, A. O. Macchiavelli, C. M. Parry, G. J. Schmid, J. M. Sears, J. F. Smith, F. S. Stephens, K. Vetter, and S. Frauendorf, Phys. Rev. C **61**, 011301(R) (1999).
[16] C. J. Chiara, S. J. Asztalos, B. Busse, R. M. Clark, M. Cromaz, M. A. Deleplanque, R. M. Diamond, P. Fallon, D. B. Fossan, D. G. Jenkins, S. Juutinen, N. S. Kelsall, R. Krücken, G. J. Lane, I. Y. Lee, A. O. Macchiavelli, R. W. MacLeod, G. Schmid, J. M. Sears, J. F. Smith, F. S. Stephens, K. Vetter, R. Wadsworth, and S. Frauendorf, Phys. Rev. C **61**, 034318 (2000).
[17] F. Brandolini, M. Ionescu-Bujor, N. H. Medina, R. V. Ribas, D. Bazzacco, M. De Poli, P. Pavan, C. Rossi-Alvarez, G. de Angelis, S. Lunardi, D. De Acuña, D. R. Napoli, and S. Frauendorf, Phys. Lett. B **338**, 468 (1996).
[18] A. K. Singh, N. Nenoff, D. Roßbach, A. Görgen, S. Chmel, F. Azaiez, A. Astier, D. Bazzacco, M. Belleguic, S. Bouneau, C. Bourgeois, N. Buforn, B. Cederwall, I. Deloncle, J. Domscheit, F. Hannachi, K. Hauschild, H. Hübel, A. Korichi, W. Korten, T. Kröll, Y. LeCoz, A. Lopez-Martens, R. Lucas, S. Lunardi, H. J. Maier, E. Mergel, M. Meyer, C. Petrache, N. Redon, P. Reiter, C. Rossi-Alvarez, G. Schönwaßer, O. Stezowski, P. G. Thirolf, and A. N. Wilson, Nucl. Phys. **A707**, 3 (2002).
[19] J. Simpson, Z. Phys. A **358**, 139 (1997).
[20] J. C. Bacelar, R. M. Diamond, E. M. Beck, M. A. Deleplanque, J. Draper, and F. S. Stephens, Phys. Rev. C **35**, 1170 (1987).
[21] J. Gascon, C.-H. Yu, G. B. Hagemann, M. C. Carpenter, J. M. Espino, Y. Iwata, T. Komatusubara, J. Nyberg, S. Ogaza, G. Sletten, P. O. Tjøm, D. C. Radford, J. Simpson, A. Alderson, M. A. Bentley, P. Fallon, P. D. Forsyth, J. W. Roberts, and J. F. Sharpey-Schafer, Nucl. Phys. **A513**, 344 (1990).
[22] L. C. Northcliffe and R. F. Schilling, Nucl. Data, Sect. A **7**, 233 (1970).
[23] J. Lindhard, M. Scharff, and H. E. Schiott, Mat. Fys. Medd. K. Dan. Vidensk. Selsk. **33**, 14 (1963).
[24] R. S. Hager and E. C. Seltzer, Nucl. Data, Sect. A **4**, 1 (1968).
[25] S. Zywietz, H. Grawe, H. Haas, and M. Menningen, Hyperfine Interact. **9**, 109 (1981).